RTK and PPK: GNSS-Technologies for direct georeferencing of UAV image flights

Heinz-Jürgen PRZYBILLA, Germany and Manfred BÄUMKER, Germany

Key words: RTK, PPK, direct georeferencing, UAV photogrammetry, test field

SUMMARY

The UAV DJI Phantom 4 (and predecessor) has been available on the market for more than 10 years and is equipped with a 2-frequency GNSS receiver in its current version "RTK". In combination with a reference station or alternatively, e.g. by using the German SAPOS correction service, precise positioning in Real-Time Kinematic (RTK) mode is possible. As the system also provides raw data in RINEX format, it is also possible to determine the position using PPK (Post-Processed Kinematic). This offers extended possibilities for georeferencing UAV image flights.
This paper investigates the geometric accuracy of UAV image blocks flown with four DJI Phantom 4 RTK systems under defined conditions on the UAV test field "Zeche Zollern". The following evaluations were performed with identical parameterization by the software Agisoft Metashape. The present results show the partly strong variations in the quality of the measured RTK positions as well as their effects on the image orientation and involved parameters. A final comparison between the use of RTK measurements and those from post-processing (PPK) does not show a noticeable gain in accuracy for the investigated image blocks.

ZUSAMMENFASSUNG

Das UAV DJI Phantom 4 (und Vorläufer) ist seit mehr als 10 Jahren im Markt verfügbar und ist in seiner aktuellen Version „RTK“ mit einem 2-Frequenz GNSS-Empfänger ausgestattet. In Verbindung mit einer Referenzstation oder alternativ z.B. durch die Nutzung des deutschen SAPOS-Dienstes ist eine präzise Positionsbestimmung im Realtime Kinematic Modus möglich. Da das System auch Rohdaten im RINEX-Format zur Verfügung stellt, kann grundsätzlich auch eine Positionsbestimmung mittels PPK (Post-Processed Kinematic) durchgeführt werden. Hieraus ergeben sich erweiterte Möglichkeiten zur Georeferenzierung von UAV-Bildflügen.
Im Beitrag erfolgen Untersuchungen zur geometrischen Genauigkeit von UAV-Bildverbänden, die mit vier DJI Phantom 4 RTK Systemen unter definierten Bedingungen auf dem UAV-Testfeld „Zeche Zollern“ geflogen wurden. Die Auswertungen erfolgten mit identischer Parametrisierung durch die Software Agisoft Metashape. Die vorliegenden Ergebnisse zeigen die zum Teil starken Variationen in der Qualität der gemessenen RTK-Positionen sowie deren Auswirkungen auf die Bildorientierung und beteiligte Parameter. Ein abschließender Vergleich zwischen der Nutzung der RTK-Messungen und solchen aus einem Post-Processing (PPK) zeigt für die untersuchten Bildverbände keinen erkennbaren Genauigkeitsgewinn.

RTK and PPK: GNSS-Technologies for direct georeferencing of UAV image flights

Heinz-Jürgen PRZYBILLA, Germany and Manfred BÄUMKER, Germany

1. INTRODUCTION

Unmanned Aerial Vehicles (UAV) are enjoying increasing popularity in the geodetic-photogrammetric community. The market - with complete systems offered by various manufacturers - is growing steadily. The Chinese supplier Da-Jiang Innovations Science and Technology Co, Ltd (DJI) is the market leader, with a current share of approx. 70% of the global consumer UAV market (Handelsblatt 2020). The Phantom 4 model (and its predecessor) has been available for more than 10 years and is equipped with a 2-frequency GNSS receiver in its current "RTK" version (Fig. 1).

Fig. 1: DJI Phantom 4 RTK

In connection with a reference station or alternatively through the connection via NTRIP (Network Transport of RTCM via Internet Protocol) via mobile radio or Wi-Fi hotspot, it is possible, for example (in Germany), to use the SAPOS service (SAPOS 2020), and thus precise positioning in real-time. The manufacturer's specifications (DJI 2020) for positioning accuracy are

- Vertical: 1.5 cm + 1 ppm (RMS)
- Horizontal: 1 cm + 1 ppm (RMS)

Since the system also provides raw data in RINEX format (Receiver Independent Exchange Format), it is also possible to determine positions using PPK (Post-Processed Kinematic). The GNSS raw data of a dual-frequency receiver (code and carrier phase observations as well as the ephemeris data) are the basis for subsequent evaluation, which usually leads to the determination of position solutions of higher accuracy. The user is thus offered extended possibilities for georeferencing UAV image flights. In addition to (indirect) orientation using ground control points (GCP), both, direct georeferencing using measured image positions (exterior orientation – EO) and a combination of the two approaches (integrated orientation) is possible.

Within the scope of this contribution, investigations on the geometric accuracy of UAV image blocks are carried out. For this purpose 4 different DJI Phantom 4 RTK systems were flown on the area of the precision UAV test field of the industrial museum "Zeche Zollern" in Dortmund, Germany (position and height accuracy of the control points approx. 2 mm; Przybilla et al. 2018). All image flights were carried out with a fixed configuration (cross-flight pattern with 20% height difference, longitudinal coverage 80%, cross coverage 60%, GSD 14 mm, manual focusing (MF) of the camera to infinity) on three different days.

2. RTK IMAGE FLIGHT

The planning and execution of the image flight with a DJI RTK copter system is carried out using a self-contained software package from the manufacturer (DJI GS PRO), which also contains the specifications for obtaining the GNSS correction data (Fig. 2).

Fig. 2: Definition of RTK parameters using the GS PRO App (Image: Manufacturer)

During the image flight for each image a frame number, a time stamp, the components of the lever arm between the antenna center and the image center of the CMOS sensor, the complete position data (in WGS84 or ETRS89 when using the SAPOS service HEPS), associated accuracy information and the RTK status are logged (Fig. 3).

137007.745028	[2074]	26,N	2,E	191,V	51.51629799,Lat	7.33605200,Lon	219.190,Ellh	0.011534,	0.014892,	0.023045	50,Q
137011.540180	[2074]	39,N	-11,E	190,V	51.51634436,Lat	7.33592497,Lon	219.164,Ellh	0.011257,	0.014774,	0.022825	50,Q
137014.828655	[2074]	37,N	-13,E	190,V	51.51639034,Lat	7.33580400,Lon	219.238,Ellh	0.010862,	0.014808,	0.022815	50,Q
137018.129651	[2074]	42,N	-17,E	189,V	51.51643734,Lat	7.33568114,Lon	219.209,Ellh	0.010905,	0.014635,	0.022773	50,Q
137021.436674	[2074]	43,N	-13,E	189,V	51.51648456,Lat	7.33555970,Lon	219.129,Ellh	0.011128,	0.014976,	0.022773	50,Q
137024.768855	[2074]	44,N	-13,E	189,V	51.51653165,Lat	7.33543664,Lon	219.082,Ellh	0.011046,	0.014868,	0.022922	50,Q
137028.065583	[2074]	44,N	-18,E	189,V	51.51657771,Lat	7.33531410,Lon	219.076,Ellh	0.011286,	0.015268,	0.023078	50,Q
137031.362426	[2074]	43,N	-19,E	189,V	51.51662397,Lat	7.33519211,Lon	219.114,Ellh	0.011445,	0.015365,	0.023139	50,Q
137034.646846	[2074]	42,N	-13,E	190,V	51.51667034,Lat	7.33507188,Lon	219.140,Ellh	0.011212,	0.015130,	0.022813	50,Q
137037.943424	[2074]	43,N	-16,E	189,V	51.51671679,Lat	7.33494892,Lon	219.147,Ellh	0.011580,	0.015509,	0.023134	50,Q

Fig 3: Extract from Timestamp.MRK system-file with logged RTK information

It should be noted here that the definition of the lever arm - as a vector between the antenna centre and the projection centre - differs from the usual definition in photogrammetry! Furthermore, the original satellite observation data as well as the ephemeris data are collected and stored in a PPKRAW.bin file in RTCM 3.2 format. Additionally, the system converts the satellite data on the fly into the RINEX format (Receiver Independent Exchange Format) and writes these data into a RINEX.obs file. This also provides all relevant information for a PPK

evaluation. This can be carried out on demand, e.g. on the basis of the free RTKLIB software (Bäumker 2014, Takasu 2020).
For further processing, the available position data must usually be converted into a target coordinate system, in Germany often into the national coordinate system ETRS89. Since the height information is available as ellipsoid coordinates after the flight a geoid undulation (currently in GCG2016 - German Combined Quasigeoid Model) must also be applied as a correction term. As a result heights in the German Main Altitude Network DHHN2016 are calculated. "The horizontal variations" of the quasi-geoid can take amounts up to 10 mm per km. Quasigeoid variations must therefore also be taken into account in local height determinations, e.g. when using GNSS" (BKG 2020a). In addition to a web application (BKG 2020b), BKG also sells a software as a desktop solution to solve this task.

3. RESEARCH RESULTS

The following evaluations were carried out for four different Phantom 4 RTK systems, which were used on three different days. The evaluations were performed with the software Agisoft Metashape. All calculations are based on identical parameterization to ensure comparability of the results.

3.1 Quality of RTK measurements

If the georeferencing of a bundle block is to be carried out using measured exterior orientations, the question concerning the quality of the measured position data must first be clarified. The manufacturer's specifications listed in chapter 1 regarding the achievable accuracies are in a range that requires both, an optimal satellite configuration and an undisturbed reception of the real-time correction data. It is not possible to assume these basic conditions in their entirety. The manufacturer names four different quality levels for the RTK status, which is also displayed in the control app during the image flight (Fig. 2 right):

- None
- RTK-FIX (ambiguities / ambiguities solved)
- RTK-FLOAT (no solution of ambiguities)
- SINGLE-GNSS

Fig. 4 shows the standard deviations of the RTK measurements achieved during the image flights (each of which consists of two partial flights of a cross-flight pattern). The present results show the partly strong variations in the quality of the measured RTK positions. Only the measurements of system A show a homogeneous data quality corresponding to a FIX solution. A small number of visible satellites, a bad geometry of the satellite constellation and a bad radio link between base station and rover can prevent a FIX solution.
The main factor influencing the data in this case is the quality of the data connection to the SAPOS service HEPS. Problems of this type are not untypical and are caused by the poor quality of the mobile network. However, atmospheric influences can also be a reason. For example, the cross-flight with system D took place under unfavorable weather conditions (wind, rising rain front). For the flights with systems B and C, the RTK quality is acceptable for one partial flight each, while for the second partial flight there are significant fluctuations in accuracy. The flights with system A show a consistently high RTK quality.

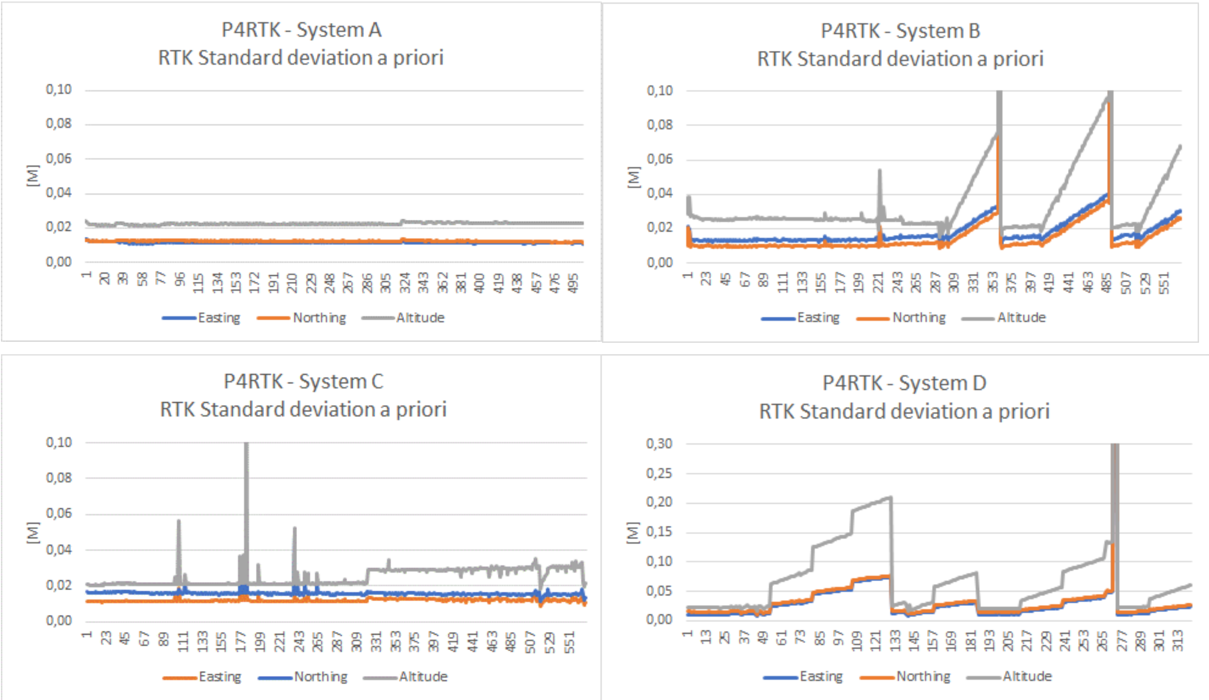

Fig. 4: Standard deviations (à priori) of the image positions determined by RTK (measured EO) of the Phantom 4 RTK systems A - D.
Note: the vertical scaling for system D differs from that of systems A - C.

3.2 Georeferencing of the image blocks using RTK

The RTK measurements shown in Chapter 3.1 can be used as a basis for image orientation within the framework of bundle block adjustment (BBA), with the aim of reducing the number of necessary control points or even completely dispensing with them (Przybilla et al. 2015, Gerke & Przybilla 2016).

The following investigations are based on typical configurations, which result from a combination of control points and measured exterior orientation (integrated orientation). In contrast to image blocks of man-bearing aerial photogrammetry, sufficiently accurate measurements of the orientation angles, as provided by a high-precision inertial measurement system, are not available here. The configurations listed in Tab. 1 have been evaluated. Depending on the individual block, the maximum number of GCP varies between 45 and 50. For all configurations a uniform interior orientation (UNIFIED) was introduced for the two partial flights of the cross-flight pattern. A further calculation was performed with two separate interior orientations (SEPARATE) for georeferencing with observed EO and 4 GCP in the block corners. The aim of this variant is to detect a possible influence of changing camera focus.

Tab. 1: Orientation configurations based on measured EO and control points

Interior Orientation (IO)	EO	Maximum GCP (45-50)	4 GCP in the block corners	EO & 4 GCP	EO & 1 GCP
UNIFIED	X	X	X	X	X
SEPARATE	-	-	-	X	-

The RTK data collected during the image flights with the DJI systems were introduced into the BBA as observations with their à priori accuracies. In addition, the influence of different control point configurations was evaluated. Fig. 5 shows the residuals of the observed exterior orientations after the bundle adjustment.

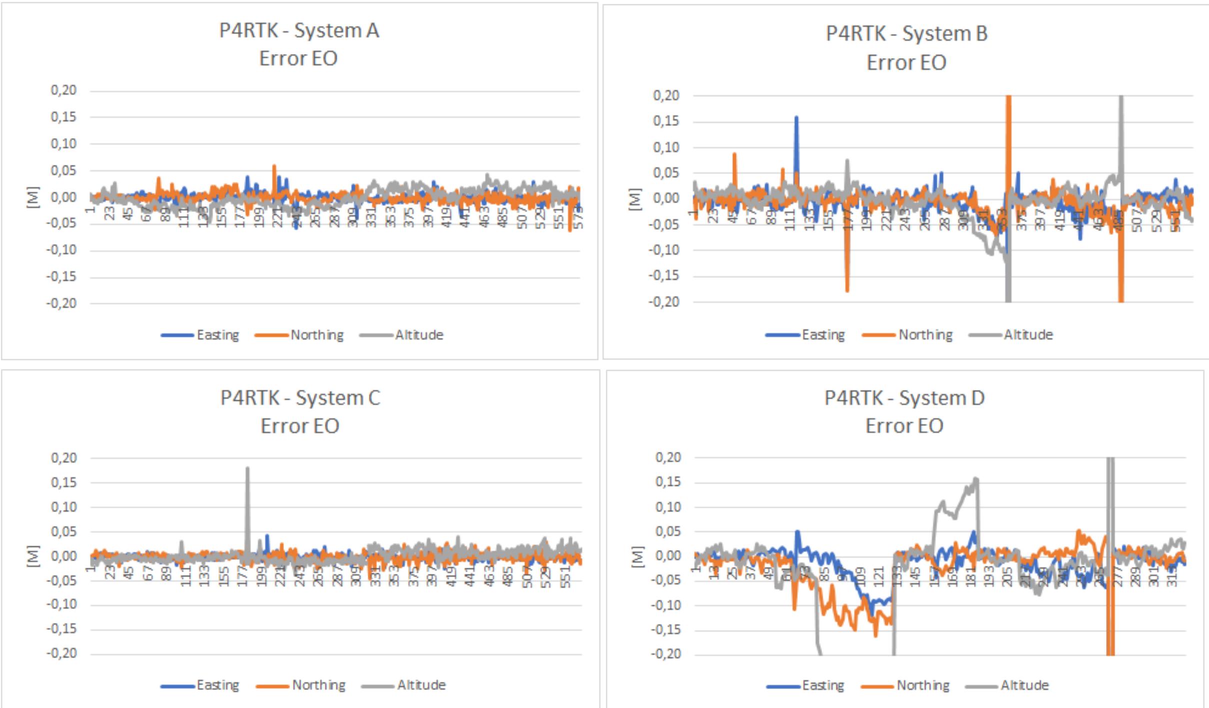

Fig. 5: Residuals (Error) at the image positions determined by RTK (EO) after the BBA for the systems A - D

In Agisoft Metashape these parameters are called "ERROR". The results shown in the figure are based on a geodetic datum consisting of the RTK measurements and additional 4 control points in the block corners. The residuals are in the order of magnitude of the observation accuracies (system A and C) for image flights with a high proportion of FIX solutions. The results for systems B and D indicate the (partially) systematically bad RTK measurements by correspondingly high residuals.
The check of the block geometry, here in particular also of block deformations, is carried out via the residuals (RMSE) at the control points (checkpoints – CP, Fig. 7). In contrast, the corresponding RMSE values at the control points (Ground Control Points – GCP, Fig. 6) are less meaningful. They merely reflect how the screen layout is adapted to GCP.

RMSE GCP - Phantom 4 RTK System A / MF

	EO	45 GCP (IO UNIFIED)	4 GCP (IO UNIFIED)	EO & 4 GCP (IO UNIFIED)	EO & 1 GCP (IO UNIFIED)	EO & 4 GCP (IO SEPARATE)
X-Error	-	10,3	2,6	8,2	7,3	6,6
Y-Error	-	6,2	2,2	7,2	1,5	6,5
Z-Error	-	6,1	9,6	10,8	27,6	6,5
3D-Error	-	13,5	10,2	15,4	28,6	11,3

RMSE GCP - Phantom 4 RTK System B / MF

	EO	49 GCP (IO UNIFIED)	4 GCP (IO UNIFIED)	EO & 4 GCP (IO UNIFIED)	EO & 1 GCP (IO UNIFIED)	EO & 4 GCP (IO SEPARATE)
X-Error	-	4,9	2,7	8,3	2,0	7,5
Y-Error	-	6,6	5,0	7,0	4,4	8,1
Z-Error	-	7,8	4,6	7,6	0,1	7,6
3D-Error	-	11,4	7,3	13,3	4,9	13,4

RMSE GCP - Phantom 4 RTK System C / MF

	EO	49 GCP (IO UNIFIED)	4 GCP (IO UNIFIED)	EO & 4 GCP (IO UNIFIED)	EO & 1 GCP (IO UNIFIED)	EO & 4 GCP (IO SEPARATE)
X-Error	-	4,6	3,3	15,3	10,9	14,5
Y-Error	-	6,1	3,3	12,8	17,1	13,1
Z-Error	-	5,9	10,0	11,3	14,1	9,0
3D-Error	-	9,7	11,0	22,9	24,7	21,5

RMSE GCP - Phantom 4 RTK System D / MF

	EO	50 GCP (IO UNIFIED)	4 GCP (IO UNIFIED)	EO & 4 GCP (IO UNIFIED)	EO & 1 GCP (IO UNIFIED)	EO & 4 GCP (IO SEPARATE)
X-Error	-	4,3	2,7	8,0	7,8	7,8
Y-Error	-	4,0	2,4	11,8	17,7	7,7
Z-Error	-	7,0	1,0	5,7	5,1	6,4
3D-Error	-	9,1	3,8	15,4	20,1	12,4

Fig. 6: RMSE values at the control points (CP) depending on the type of orientation (direct: ÄORI – indirect: GCP – integrated: ÄORI+GCP) (systems A - D)

RMSE CP - Phantom 4 RTK System A

	EO	45 GCP (IO UNIFIED)	4 GCP (IO UNIFIED)	EO & 4 GCP (IO UNIFIED)	EO & 1 GCP (IO UNIFIED)	EO & 4 GCP (IO SEPARATE)
X-Error	11,3	-	14,3	11,7	11,3	11,4
Y-Error	9,8	-	10,5	9,2	10,0	8,7
Z-Error	145,9	-	243,3	12,3	29,8	9,6
3D-Error	146,7	-	244,0	19,3	33,4	17,2

RMSE CP - Phantom 4 RTK System B

	EO	49 GCP (IO UNIFIED)	4 GCP (IO UNIFIED)	EO & 4 GCP (IO UNIFIED)	EO & 1 GCP (IO UNIFIED)	EO & 4 GCP (IO SEPARATE)
X-Error	6,1	-	13,0	5,5	6,2	5,5
Y-Error	8,6	-	16,9	8,3	8,6	8,4
Z-Error	15,6	-	445,7	14,2	15,0	17,5
3D-Error	18,8	-	446,2	17,3	18,4	20,2

RMSE CP - Phantom 4 RTK System C

	EO	49 GCP (IO UNIFIED)	4 GCP (IO UNIFIED)	EO & 4 GCP (IO UNIFIED)	EO & 1 GCP (IO UNIFIED)	EO & 4 GCP (IO SEPARATE)
X-Error	12,2	-	8,7	10,1	13,7	12,3
Y-Error	15,5	-	9,1	13,7	14,3	14,2
Z-Error	87,5	-	269,4	8,5	16,1	11,1
3D-Error	89,6	-	269,7	19,0	24,8	20,6

RMSE CP - Phantom 4 RTK System D

	EO	50 GCP (IO UNIFIED)	4 GCP (IO UNIFIED)	EO & 4 GCP (IO UNIFIED)	EO & 1 GCP (IO UNIFIED)	EO & 4 GCP (IO SEPARATE)
X-Error	9,0	-	8,3	6,4	10,4	6,7
Y-Error	24,0	-	12,9	13,0	18,9	8,2
Z-Error	114,5	-	247,7	8,7	14,4	9,1
3D-Error	117,3	-	248,2	16,9	25,9	14,0

Fig. 7: RMSE values at the control points (CP) as a function of the orientation type (direct: EO – indirect: GCP – integrated: EO+GCP) (systems A - D).
Note: the vertical scaling differs from that of GCP (Fig. 6) by a factor of 10.

Fig. 7 shows very clearly the influences of the type of orientation on the respective block. The following effects can be derived:

- Direct orientation using measured EO
  The deviations at the CP are, in relation to the ground coordinates, in the magnitude of the RTK accuracy (10-20 mm), but a significantly large deviation in height is shown. This is well over 100 mm for systems A and D and just under this value for system C. Only for system B the deviation is within the range of the observation accuracy. A reliable georeferencing for this variant (without ground control points) is not recognizable.
- Indirect orientation with maximum number of control points
  As all GCP are used for referencing in this variant, it is not possible to control the system using independent CP. However, Fig. 6 shows the high quality of the adjustment to GCP, which is approx. 0.5 - 0.7 of the GSD. The variant considered here is associated with a very high terrestrial effort.
- Indirect orientation with minimum number of control points
  From the georeferencing using 4 GCP in the block corners it is clearly visible that no sufficient stability can be achieved in the image blocks. While the ground deviations of the CP are still within the range of the GSD, the height deviations exceed these by a factor of 15 - 30. One reason for this result can be seen in the metric of the camera and the obviously insufficient possibilities for a simultaneous self-calibration (chapter 3.3).
- Integrated orientation using measured EO and four control points
  The present results show the effectiveness of the integrated orientation based on the RTK measurements in conjunction with control points in the block corners. The deviations at the CP are within the range of the GSD, in some cases even below. The results obtained are only slightly worse than the variant with a full control point referencing.
- Integrated orientation using measured EO and one control point
  While direct orientation by means of measured exterior orientation is characterized by significant height deviations in the available data sets, the positive effects of an additional control point (in the middle of the block) are clearly visible. The systematic height deviations at the CP are reduced to approx. 15 - 30 mm and are thus on the same level of accuracy as the RTK measurements. The quality of the image orientation accuracy achieved here is sufficient for e. g. topographic applications.

3.3 Georeferencing of the image blocks using Post-Processed Kinematic (PPK)

DJI RTK systems offer, due to the availability of the original satellite observation data as well as ephemeris data, the possibility of an improved position determination in post-processing (PPK). The necessary calculations can be performed using the free software RTKLIB (Takasu 2020). Since DJI does not have its own evaluation software, RTKLIB is used in the workflows of various third-party providers (Aerotas 2020, KlauPPK 2020). General information on GNSS workflows can be found, for example, in EMLID (2020). Special attention should be paid to the correct adjustment/interpolation of the positioning data to the respective time stamp of the image acquisition as well as to the lever arm correction. The software required for this was developed by Bäumker (2020) and used for post-processing.

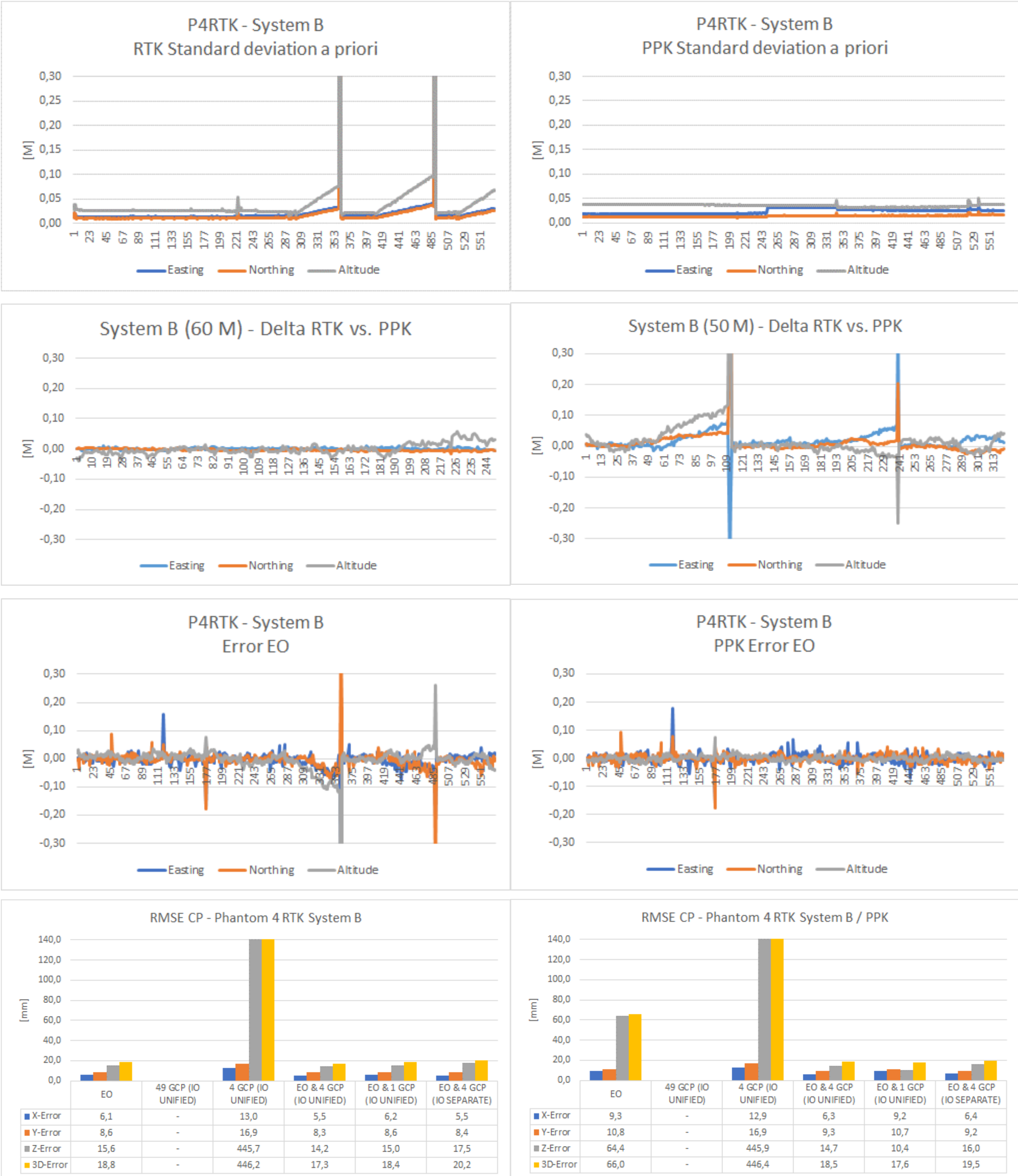

Fig. 8: Comparison of evaluations based on RTK (left) and PPK (right) for system B:
Top: Standard deviations (à priori) of the determined image positions (EO)
Middle-up: Differences between RTK and PPK (left: flight 1, right: flight 2)
Middle-down: Residuals (Error) at the image positions (EO) after the BBA
Bottom: RMSE values at the control points (CP) depending on the type of orientation

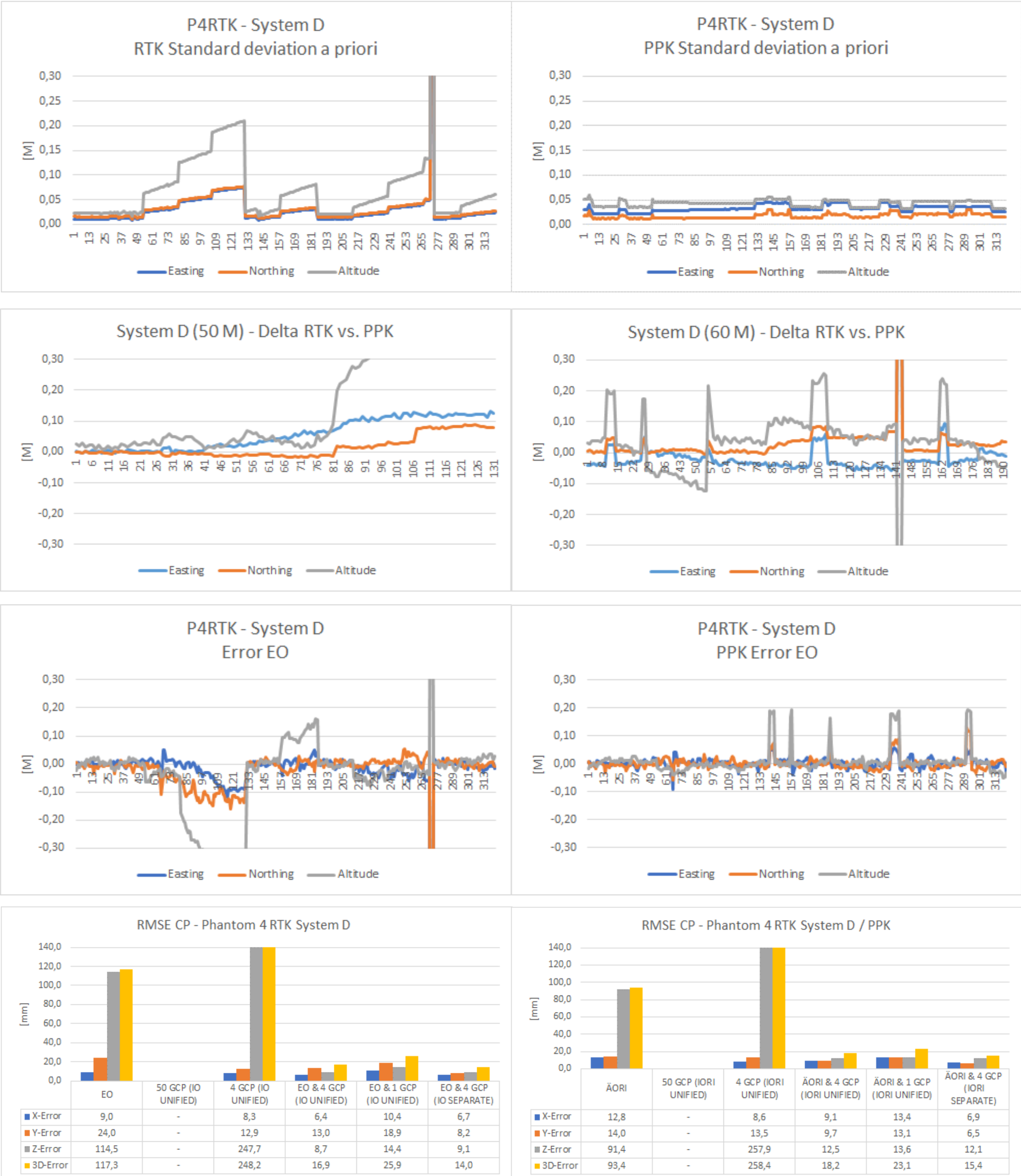

	EO	50 GCP (IO UNIFIED)	4 GCP (IO UNIFIED)	EO & 4 GCP (IO UNIFIED)	EO & 1 GCP (IO UNIFIED)	EO & 4 GCP (IO SEPARATE)
X-Error	9,0	-	8,3	6,4	10,4	6,7
Y-Error	24,0	-	12,9	13,0	18,9	8,2
Z-Error	114,5	-	247,7	8,7	14,4	9,1
3D-Error	117,3	-	248,2	16,9	25,9	14,0

	ÄORI	50 GCP (IORI UNIFIED)	4 GCP (IORI UNIFIED)	ÄORI & 4 GCP (IORI UNIFIED)	ÄORI & 1 GCP (IORI UNIFIED)	ÄORI & 4 GCP (IORI SEPARATE)
X-Error	12,8	-	8,6	9,1	13,4	6,9
Y-Error	14,0	-	13,5	9,7	13,1	6,5
Z-Error	91,4	-	257,9	12,5	13,6	12,1
3D-Error	93,4	-	258,4	18,2	23,1	15,4

Fig. 9: Comparison of evaluations based on RTK (left) and PPK (right) for system D:

Top: Standard deviations (à priori) of the determined image positions (EO)
Middle-up: Differences between RTK and PPK (left: flight 1, right: flight 2)
Middle-down: Residuals (Error) at the image positions (EO) after the BBA
Bottom: RMSE values at the control points (CP) depending on the type of orientation

Fig. 8 shows comparative data (system B) from RTK and PPK processing. It becomes clear that the observations with large standard deviations à priori, which occur repeatedly in RTK, are essentially no longer present in PPK processing. However, it remains recognizable that in the second partial flight (image number from approx. 245, flight altitude above ground: 50 m) – in comparison to the first (flight altitude above ground: 60 m) – an obviously worse satellite configuration was present, which leads to a worse observation accuracy. The differences between RTK and PPK evaluation show a good agreement in wide ranges, but there are also partial problems with the position determination.

The residuals (ERROR) at the image positions after the BBA are very similar in many areas, which speaks for the overall good RTK solution. This result is also confirmed by the residual at the control points. The results are almost identical for all georeferencing types. Only the direct orientation using measured EO shows differences, with surprisingly higher RMSE values for the PPK solution.

The comparative RTK vs. PPK data for system D is shown in Fig. 9. The available RTK data show à priori accuracies >10 cm for approx. 20% of totally 321 images of the flight. It can be assumed that no FIX solution is present here (Fig. 10). The flight shows the worst RTK quality compared to those of systems A - C. The PPK solution provides lower accuracies than that of system B. Although these are almost homogeneous in ground and height when the two partial flights are considered separately, they are noticeably worse in the second partial flight (60 m). More frequent, larger differences between RTK and PPK evaluation are the result (Fig. 9, middle-up).

The general quality gain of the PPK solution is not reflected in the results after the BBA. Despite the homogeneous quality of the position determinations, there are errors of up to 20 cm in the measured EO for various areas of the image block. The reasons may be a bad satellite configuration in conjunction with very unfavourable weather conditions at the time of the image flight. Fig. 11 shows clear systematics for the additional values made to the EO in the context of the BBA.

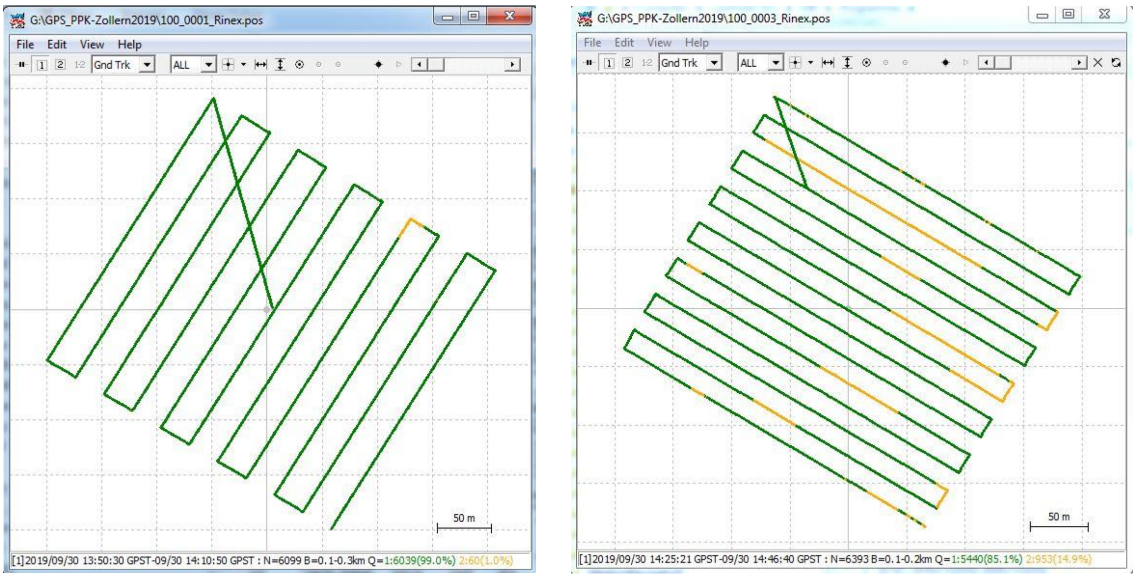

Fig 10: Share of FIX (green) and FLOAT solutions (yellow) from post-processing with RTKLIB for flights with system D (flight altitude above ground, left 50 m, right 60 m

The final comparison of the RMSE values at the control points (Fig. 9 bottom) provides almost identical results. The presumed gain in accuracy through post-processing is not detectable in the present data set.

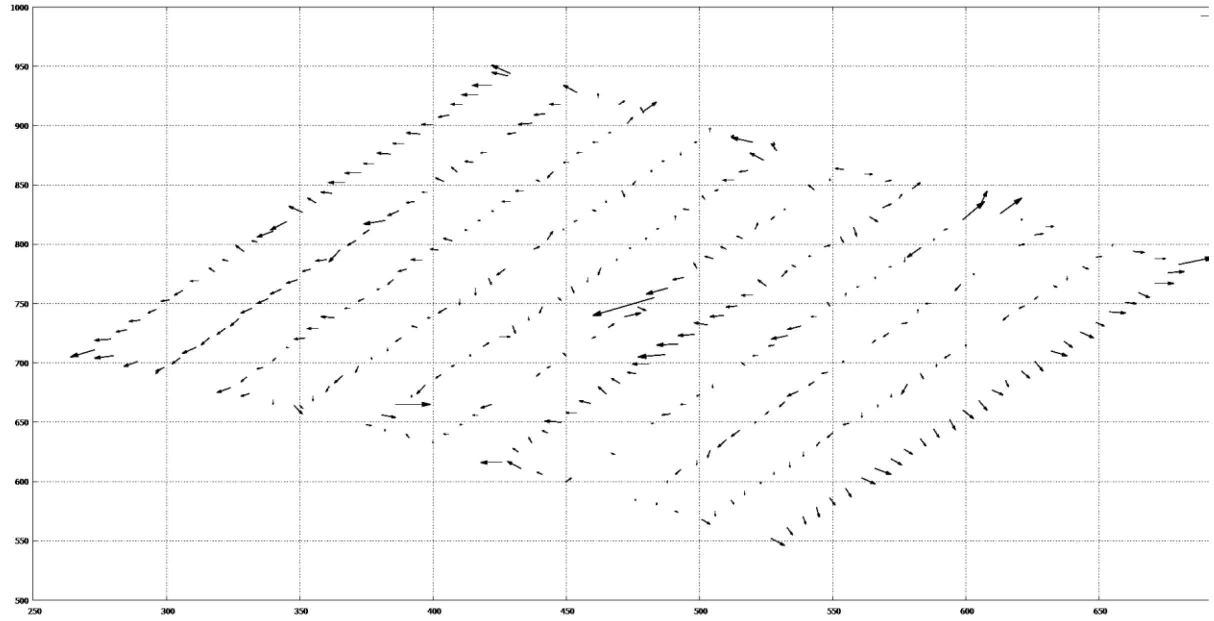

RMSE values: Easting:19,3 mm, Northing: 20,1 mm (not shown: Altitude: 26,4 mm)

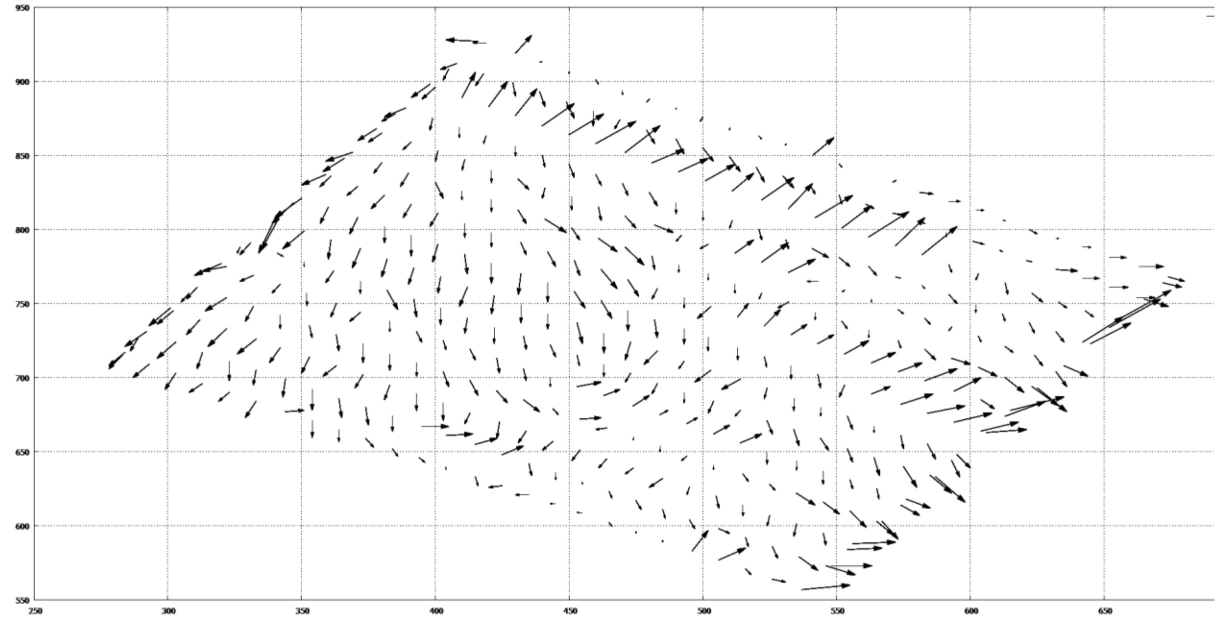

RMSE values: Easting: 29,9 mm, Northing: 45,2 mm (not shown: Altitude: 74,5 mm)
Fig. 11: RMSE values of the EO according to BBA (indirect orientation using 50 GCP), with clearly recognizable systematics in the PPK measurements. System D - Flight altitude above ground: Top 50 m, Bottom 60 m.

3.4 Interior orientation of the camera

Prerequisite for the in-situ calibration of the camera in the BBA is, in addition to a suitable recording configuration (here: cross-flight pattern), the availability of corresponding referencing information (control points, measured elements of the EO). Fig. 12 shows changes of the parameters focal length (Δc) and principal point (XH, YH) depending on the block orientation. For all cameras there are small changes in the principal point (< 1 pixel), a result that shows the high stability of the respective systems.

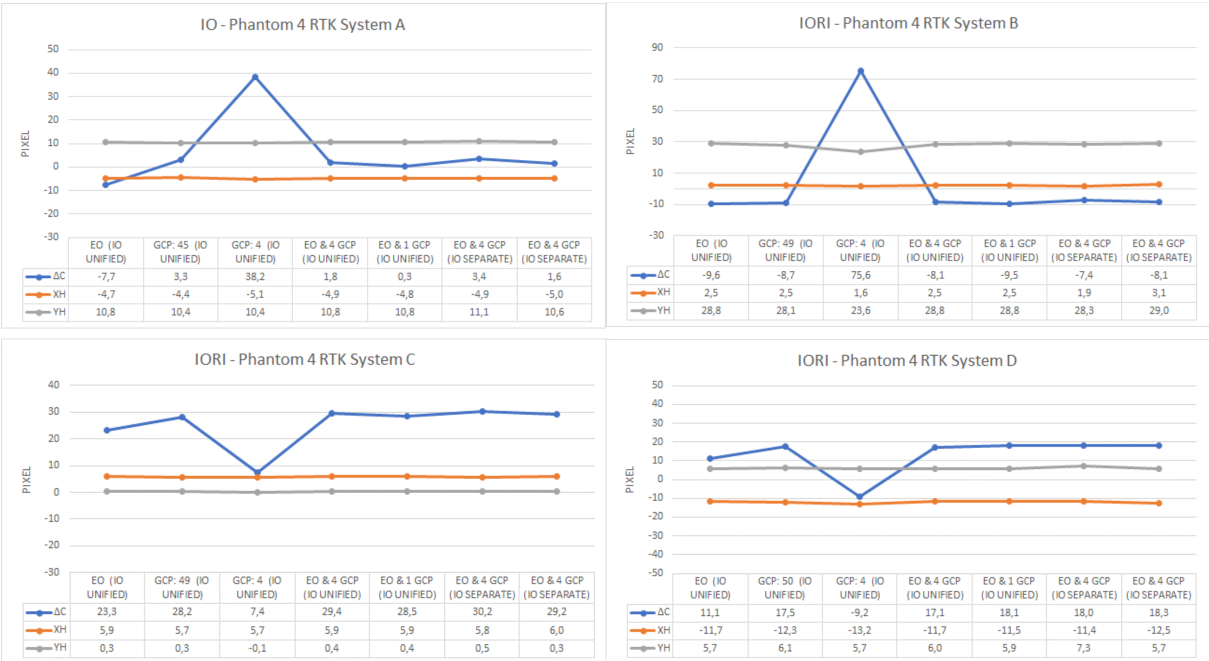

Fig. 12: Changes of the parameters of the interior orientation (Δc, XH, YH) depending on the block orientation as well as common or separate parameters for the partial flights (systems A - D).
Note: the deviations Δc refer to a uniform start value.

The influence of the block orientation on the parameter "focal length" is very clear in all systems. When using only four control points in the block corners, a reliable determination of this parameter is not possible. The deviations compared to all other variants are between 20 - 80 pixels. The corresponding (negative) consequences are shown in fig. 7, here especially with the shown height deviations at the control points.
The used approaches of a common (UNIFIED) or separate (SEPARATE) parametrization of the interior orientation for the respective partial flights show nearly identical results, both for the RMSE values at the control points (Fig. 7) and for the variation of the focal length (Fig. 8). From this it can be deduced that a stability of the examined parameters can be assumed for the course of the two partial flights of the cross-flight pattern.

4. CONCLUSION & OUTLOOK

With the availability of precise RTK solutions for UAV image flight and the associated direct georeferencing of photogrammetric image blocks, an important step has been taken with regard to the economic use of UAVs in geodesy and photogrammetry. The Phantom 4 RTK UAV systems investigated in this article provide sufficient possibilities for applications in the medium accuracy range (> 2 - 3 cm) to significantly reduce the terrestrial effort for georeferencing by eliminating extensive control point measurements as far as possible. However, the present results also show the partly strong variations in the quality of the measured RTK positions and their effects on the image orientation and the parameters involved. A georeferencing exclusively using the measured elements of the exterior orientation does not seem to make sense according to the available results, since systematic height offsets are often recognizable. The integrated orientation approach is the method of choice here. Table 2 contains a proposal for the use of RTK / PPK, depending on typical applications.

Tab. 2: Use of RTK and PPK depending on the application

Parameter	Topography	Cadastre	Engineering Survey
GSD	2,5 cm	1,5 cm	< 1cm
Image scale	1:10.000	1:5.000	1:1.000
Accuracy range	10 - 20 cm	1 - 3 cm	0,2 - 1 cm
Achievable accuracy	+++	++	+
Orientation	RTK / PPK	RTK / PPK & GCP*	GCP**
Point cloud	x	x	x
Volumes	x	-	-
Contour lines	x	-	-
Profile	x	-	x
Orthophoto	x	x	-
Map	x	x	-
3D Points	-	x	x

GCP* - GNSS measurement / GCP** - Network measurement

The post-processing of the GNSS data, which required additional effort, did not provide any additional gain in accuracy for the two P4RTK data sets investigated here, although no FIX solutions could be achieved for approx. 20% of the RTK data of System D. Due to an adjusted weighting (based on the à priori accuracies) in the BBA the influence of these observations is small, negative effects on the block geometry are not visible. However, the PPK solution is of significant importance wherever a poor mobile radio infrastructure prevents the use of real-time correction services. Problems of limited satellite reception cannot be compensated by the PPK either.

The quality of the camera is to be evaluated positively. The concept of the system used in the Phantom 4 RTK is identical to that of the Zenmuse X4S. The camera has a high level of stability, which is significantly higher than other systems from the manufacturer. This is due to the fixed focus lens, which eliminates mechanical instabilities caused by interchangeable optics. From the point of view of photogrammetry, despite these positive characteristics, it is not a metric camera, so an in-situ calibration is urgently required.

REFERENCES

Aerotas (2020): Phantom 4 RTK – PPK Processing Workflow. https://www.aerotas.com/phantom-4-rtk-ppk-processing-workflow. Last access: 19.01.2020

Bäumker, M. (2014): Zeitreihenanalyse der Daten der GNSS Referenzstation der Hochschule Bochum. In: Zeitabhängige Messgrößen – Ihre Daten haben (Mehr-)Wert. Beiträge zum 129. DVW-Seminar am 26. und 27. Februar 2014 in Hannover, Schriftenreihe des DVW, Band 74 (Hrsg. DVW e.V. – Gesellschaft für Geodäsie, Geoinformation und Landmanagement)

Bäumker, M. (2020): Labor für Physikalische Messtechnik der HS Bochum. https://www.hochschule-bochum.de/fbg/einrichtungen-im-fachbereich/labor-fuer-physikalische-messtechnik/. Last access: 19.01.2020

BKG (2020a): Die Höhenbezugsfläche von Deutschland. https://www.bkg.bund.de/DE/Ueber-das-BKG/Geodaesie/Integrierter-Raumbezug/Hoehenbezugsflaeche/hoehenbezug.html. Last access: 15.01.2020

BKG (2020b): Onlineberechnung von Quasigeoidhöhen mit dem GCG2016, http://gibs.bkg.bund.de/geoid/gscomp.php?p=g. Last access: 15.01.2020

DJI (2020): Phantom 4 RTK Technische Daten, https://www.dji.com/de/phantom-4-rtk/info. Last access: 15.01.2020

Emlid (2020): GPS post-processing. https://docs.emlid.com/reachm-plus/common/tutorials/gps-post-processing/. Last access: 19.01.2020

Gerke, M. & Przybilla, H.-J. (2016): Accuracy analysis of photogrammetric UAV image blocks: influence of onboard RTK-GNSS and cross flight patterns. Zeitschrift für Photogrammetrie, Fernerkundung und Geoinformation (PFG). Heft 1, 2016

Handelsblatt (2020): Diese chinesische Firma hat mit Drohnen den Massenmarkt erobert. https://www.handelsblatt.com/technik/digitale-revolution/digitale-revolution-diese-chinesische-firma-hat-mit-drohnen-den-massenmarkt-erobert/25395412.html?ticket=ST-1134012-TrivDX4ReHLfHg6nRiij-ap2. Last access: 19.01.2020

KlauPPK (2020): https://klauppk.com/klauppk-software-for-the-phantom4-rtk-2/. Last access: 19.01.2020

Przybilla, H.-J., Reuber, C., Bäumker, M. & Gerke, M. (2015): Untersuchungen zur Genauigkeitssteigerung von UAV-Bildflügen. – 35. Wissenschaftlich-Technische Jahrestagung der DGPF 24: 45–54.

Przybilla, H.-J., Bäumker, M. & Vieten, J. (2018): Das UAV-Testfeld Zeche Zollern in Dortmund. Schriftenreihe des DVW, Band 89, S. 61 – 80, Wißner-Verlag, Augsburg, ISBN: 978-3-95786-146-7

Sapos (2020): SAPOS-Dienste im Überblick. https://www.sapos.de/dienste-im-ueberblick.html. Last access: 15.01.2020

Takasu, T. (2020): RTKLIB, Open Source Program Package for RTK-GPS. http://gpspp.sakura.ne.jp/rtklib/rtklib.htm. Last access: 15.01.2020

CONTACTS

Prof. Dr. Heinz-Jürgen Przybilla
Essener Str. 117
45529 Hattingen
GERMANY
Tel. +49 160 94 98 05 79
Email: heinz-juergen@przybilla.biz
Website: https://www.researchgate.net/profile/Heinz_Juergen_Przybilla

Prof. Dr. Manfred Bäumker
Bochum University of Applied Sciences
Lennershofstr. 140
44801 Bochum
GERMANY
Tel. +49 234 32 10511
Email: manfred.baeumker@hs-bochum.de
Website: https://www.researchgate.net/profile/Manfred_Baeumker